Search for gauge mediated SUSY breaking topologies at $\sqrt{s} \sim 189$ GeV

The ALEPH Collaboration

R. Barate, D. Decamp, P. Ghez, C. Goy, S. Jezequel, J.-P. Lees, F. Martin, E. Merle, M.-N. Minard, B. Pietrzyk
Laboratoire de Physique des Particules (LAPP), IN[2]P[3]-CNRS, 74019 Annecy-le-Vieux Cedex, France

R. Alemany, S. Bravo, M.P. Casado, M. Chmeissani, J.M. Crespo, E. Fernandez, M. Fernandez-Bosman, Ll. Garrido,[15] E. Graugés, A. Juste, M. Martinez, G. Merino, R. Miquel, Ll.M. Mir, P. Morawitz, A. Pacheco, I. Riu, H. Ruiz
Institut de Física d'Altes Energies, Universitat Autònoma de Barcelona, 08193 Bellaterra (Barcelona), Spain[7]

A. Colaleo, D. Creanza, M. de Palma, G. Iaselli, G. Maggi, M. Maggi, S. Nuzzo, A. Ranieri, G. Raso, F. Ruggieri, G. Selvaggi, L. Silvestris, P. Tempesta, A. Tricomi,[3] G. Zito
Dipartimento di Fisica, INFN Sezione di Bari, 70126 Bari, Italy

X. Huang, J. Lin, Q. Ouyang, T. Wang, Y. Xie, R. Xu, S. Xue, J. Zhang, L. Zhang, W. Zhao
Institute of High Energy Physics, Academia Sinica, Beijing, P.R. China[8]

D. Abbaneo, G. Boix,[6] O. Buchmüller, M. Cattaneo, F. Cerutti, V. Ciulli, G. Davies, G. Dissertori, H. Drevermann, R.W. Forty, M. Frank, F. Gianotti, T.C. Greening, A.W. Halley, J.B. Hansen, J. Harvey, P. Janot, B. Jost, M. Kado, O. Leroy, P. Maley, P. Mato, A. Minten, A. Moutoussi, F. Ranjard, L. Rolandi, D. Schlatter, M. Schmitt,[20] O. Schneider,[2] P. Spagnolo, W. Tejessy, F. Teubert, E. Tournefier, A. Valassi, A.E. Wright
European Laboratory for Particle Physics (CERN), 1211 Geneva 23, Switzerland

Z. Ajaltouni, F. Badaud G. Chazelle, O. Deschamps, S. Dessagne, A. Falvard, C. Ferdi, P. Gay, C. Guicheney, P. Henrard, J. Jousset, B. Michel, S. Monteil, J-C. Montret, D. Pallin, J.M. Pascolo, P. Perret, F. Podlyski
Laboratoire de Physique Corpusculaire, Université Blaise Pascal, IN[2]P[3]-CNRS, Clermont-Ferrand, 63177 Aubière, France

J.D. Hansen, J.R. Hansen, P.H. Hansen,[1] B.S. Nilsson, B. Rensch, A. Wäänänen
Niels Bohr Institute, 2100 Copenhagen, Denmark[9]

G. Daskalakis, A. Kyriakis, C. Markou, E. Simopoulou, A. Vayaki
Nuclear Research Center Demokritos (NRCD), 15310 Attiki, Greece

A. Blondel, J.-C. Brient, F. Machefert, A. Rougé, M. Swynghedauw, R. Tanaka
H. Videau
Laboratoire de Physique Nucléaire et des Hautes Energies, Ecole Polytechnique, IN[2]P[3]-CNRS, 91128 Palaiseau Cedex, France

E. Focardi, G. Parrini, K. Zachariadou
Dipartimento di Fisica, Università di Firenze, INFN Sezione di Firenze, 50125 Firenze, Italy

M. Corden, C. Georgiopoulos
Supercomputer Computations Research Institute, Florida State University, Tallahassee, FL 32306-4052, USA[13,14]

A. Antonelli, G. Bencivenni, G. Bologna,[4] F. Bossi, P. Campana, G. Capon, V. Chiarella, P. Laurelli, G. Mannocchi,[1,5] F. Murtas, G.P. Murtas, L. Passalacqua, M. Pepe-Altarelli
Laboratori Nazionali dell'INFN (LNF-INFN), 00044 Frascati, Italy

M. Chalmers, J. Kennedy, J.G. Lynch, P. Negus, V. O'Shea, B. Raeven, D. Smith, P. Teixeira-Dias, A.S. Thompson, J.J. Ward
Department of Physics and Astronomy, University of Glasgow, Glasgow G12 8QQ, UK[10]

R. Cavanaugh, S. Dhamotharan, C. Geweniger,[1] P. Hanke, V. Hepp, E.E. Kluge, G. Leibenguth, A. Putzer, K. Tittel, S. Werner,[19] M. Wunsch[19]
Kirchhoff-Institut für Physik, Universität Heidelberg, 69120 Heidelberg, Germany[16]

R. Beuselinck, D.M. Binnie, W. Cameron, P.J. Dornan, M. Girone, S. Goodsir, N. Marinelli, E.B. Martin, J. Nash, J. Nowell, H. Przysiezniak,[1] A. Sciabà, J.K. Sedgbeer, J.C. Thompson,[24] E. Thomson, M.D. Williams
Department of Physics, Imperial College, London SW7 2BZ, UK[10]

V.M. Ghete, P. Girtler, E. Kneringer, D. Kuhn, G. Rudolph
Institut für Experimentalphysik, Universität Innsbruck, 6020 Innsbruck, Austria[18]

C.K. Bowdery, P.G. Buck, G. Ellis, A.J. Finch, F. Foster, G. Hughes, R.W.L. Jones, N.A. Robertson, M. Smizanska, M.I. Williams
Department of Physics, University of Lancaster, Lancaster LA1 4YB, UK[10]

I. Giehl, F. Hölldorfer, K. Jakobs, K. Kleinknecht, M. Kröcker, A.-S. Müller, H.-A. Nürnberger, G. Quast, B. Renk, E. Rohne, H.-G. Sander, S. Schmeling, H. Wachsmuth C. Zeitnitz, T. Ziegler
Institut für Physik, Universität Mainz, 55099 Mainz, Germany[16]

A. Bonissent, J. Carr, P. Coyle, A. Ealet, D. Fouchez, P. Payre, D. Rousseau, A. Tilquin
Centre de Physique des Particules, Faculté des Sciences de Luminy, IN^{2}P^3-CNRS, 13288 Marseille, France

M. Aleppo, M. Antonelli, S. Gilardoni, F. Ragusa
Dipartimento di Fisica, Università di Milano e INFN Sezione di Milano, 20133 Milano, Italy.

V. Büscher, H. Dietl, G. Ganis, K. Hüttmann, G. Lütjens, C. Mannert, W. Männer, H.-G. Moser, S. Schael, R. Settles, H. Seywerd, H. Stenzel, W. Wiedenmann, G. Wolf
Max-Planck-Institut für Physik, Werner-Heisenberg-Institut, 80805 München, Germany^p

P. Azzurri, J. Boucrot, O. Callot, S. Chen, M. Davier, L. Duflot, J.-F. Grivaz, Ph. Heusse, A. Jacholkowska,[1] J. Lefrançois, L. Serin, J.-J. Veillet, I. Videau,[1] J.-B. de Vivie de Régie, D. Zerwas
Laboratoire de l'Accélérateur Linéaire, Université de Paris-Sud, IN^{2}P^3-CNRS, 91898 Orsay Cedex, France

G. Bagliesi, T. Boccali, C. Bozzi,[12] G. Calderini, R. Dell'Orso, I. Ferrante, A. Giassi, A. Gregorio, F. Ligabue, P.S. Marrocchesi, A. Messineo, F. Palla, G. Rizzo, G. Sanguinetti, G. Sguazzoni, R. Tenchini,[1] A. Venturi, P.G. Verdini
Dipartimento di Fisica dell'Università, INFN Sezione di Pisa, e Scuola Normale Superiore, 56010 Pisa, Italy

G.A. Blair, J. Coles, G. Cowan, M.G. Green, D.E. Hutchcroft, L.T. Jones, T. Medcalf, J.A. Strong
Department of Physics, Royal Holloway & Bedford New College, University of London, Surrey TW20 OEX, UK[10]

D.R. Botterill, R.W. Clifft, T.R. Edgecock, P.R. Norton, I.R. Tomalin
Particle Physics Department, Rutherford Appleton Laboratory, Chilton, Didcot, Oxon OX11 OQX, UK[10]

B. Bloch-Devaux, P. Colas, B. Fabbro, G. Faïf, E. Lançon, M.-C. Lemaire, E. Locci, P. Perez, J. Rander, J.-F. Renardy, A. Rosowsky, P. Seager,[23] A. Trabelsi,[21] B. Tuchming, B. Vallage
CEA, DAPNIA/Service de Physique des Particules, CE-Saclay, 91191 Gif-sur-Yvette Cedex, France[17]

S.N. Black, J.H. Dann, C. Loomis, H.Y. Kim, N. Konstantinidis, A.M. Litke, M.A. McNeil, G. Taylor
Institute for Particle Physics, University of California at Santa Cruz, Santa Cruz, CA 95064, USA[22]

C.N. Booth, S. Cartwright, F. Combley, P.N. Hodgson, M. Lehto, L.F. Thompson
Department of Physics, University of Sheffield, Sheffield S3 7RH, UK[10]

K. Affholderbach, A. Böhrer, S. Brandt, C. Grupen, J. Hess, A. Misiejuk, G. Prange, U. Sieler
Fachbereich Physik, Universität Siegen, 57068 Siegen, Germany[16]

C. Borean, G. Giannini, B. Gobbo
Dipartimento di Fisica, Università di Trieste e INFN Sezione di Trieste, 34127 Trieste, Italy

J. Putz, J. Rothberg, S. Wasserbaech, R.W. Williams
Experimental Elementary Particle Physics, University of Washington, WA 98195 Seattle, USA

S.R. Armstrong, P. Elmer, D.P.S. Ferguson, Y. Gao, S. González, O.J. Hayes, H. Hu, S. Jin, J. Kile, P.A. McNamara III, J. Nielsen, W. Orejudos, Y.B. Pan, Y. Saadi, I.J. Scott, J. Walsh, J.H. von Wimmersperg-Toeller, Sau Lan Wu, X. Wu, G. Zobernig

Department of Physics, University of Wisconsin, Madison, WI 53706, USA[11]

Abstract. Searches for topologies characteristic of Gauge Mediated SUSY Breaking models (GMSB) are performed by analysing 173.6 pb^{-1} of data collected at $\sqrt{s} = 188.6$ GeV with the ALEPH detector. These topologies include acoplanar photons, non-pointing single photon, acoplanar leptons, large impact parameter leptons, detached slepton decay vertices, heavy stable charged sleptons and four leptons plus missing energy final states. No evidence for these new phenomena is observed and limits on production cross sections and sparticle masses are derived. A scan of a minimal GMSB parameter space is performed and model dependent lower limits of about 45 GeV/c^2 on the next-to-lightest supersymmetric particle (NLSP) mass and of about 9 TeV on the mass scale parameter Λ are derived, independently of the NLSP lifetime.

1 Introduction

A search for topologies that are the expected characteristic manifestations of Gauge Mediated SUSY Breaking

models [1] (GMSB) is reported in this paper. The main motivation for this class of models is the fact that they can naturally accommodate the experimentally observed absence of flavour changing neutral currents. This is due to the fact that in GMSB the mechanism that propagates the SUSY breaking to the visible sector is flavour blind (gauge interactions) and that the scale at which this happens is not too far from the electroweak and well below the Grand Unification scale.

From the phenomenological point of view the main difference with respect to Gravity Mediated SUSY Breaking models is that in GMSB the Lightest Supersymmetric Particle (LSP) is the gravitino ($\tilde{G}$), which couples very weakly to the other particles. In GMSB the natural mass range for the gravitino LSP is 10^{-2}–10^4 eV/c^2 [1]. In e^+e^- collisions, pairs of SUSY particles can be produced and subsequently decay to their SM partners plus two gravitinos (R-parity conservation is assumed). Another important feature of these models is that the next-to-lightest supersymmetric particle (NLSP) is, in general, either the lightest neutralino (χ) or the slepton ($\tilde{\ell}$). In this scenario, if the mixing in the stau sector is small the sleptons ($\tilde{e}$, $\tilde{\mu}$, $\tilde{\tau}$) are three degenerate co-NLSPs while for large mixing the stau is expected to be the NLSP. The lightest neutralino and the sleptons are expected to be much lighter than the other SUSY particles (charginos, squarks and gluinos) and therefore they are the most relevant at LEP2.

The lifetime of the NLSP depends on the gravitino mass (or equivalently on the SUSY breaking scale $\sqrt{F}$ which is proportional to it), for a given NLSP mass and field composition. For a gravitino heavier than a few hundred eV/c^2, the distance scale associated with this lifetime can be comparable to or even larger than the size of the ALEPH detector. For this reason topological searches that are able to identify a long-lived or a stable NLSP are developed.

A list of the experimental topologies searched for in this paper is given in Table 1.

The ALEPH Collaboration has previously published separate papers on some of these topologies. Analyses related to searches for photons plus missing energy, which are characteristic of the χ NLSP scenario, have been pub-

Table 1. Final state topologies studied in the different scenarios

NLSP	Production	Decay mode	Lifetime	Expected topology
χ	$e^+e^- \to \chi\chi$	$\chi \to \gamma\tilde{G}$	$c\tau << \ell_{detector}$	Acoplanar photons
			$c\tau \sim \ell_{detector}$	Non-pointing photon
			$c\tau >> \ell_{detector}$	Invisible (indirect search)
$\tilde{\ell}$	$e^+e^- \to \tilde{\ell}\tilde{\ell}$	$\tilde{\ell} \to \ell\tilde{G}$	$c\tau << \ell_{detector}$	Acoplanar leptons
			$c\tau \sim \ell_{detector}$	Kinks and large impact parameters
			$c\tau >> \ell_{detector}$	Heavy stable charged particles
$\tilde{\ell}$	$e^+e^- \to \chi\chi$	$\chi \to \tilde{\ell}\ell \to \ell\ell\tilde{G}$	$c\tau << \ell_{detector}$	Four leptons
			$c\tau \sim \ell_{detector}$	Not covered here
			$c\tau >> \ell_{detector}$	Not covered here

lished in [2] while topologies involving sleptons, which are characteristic of the $\tilde{\ell}$ NLSP scenario, have been published in [3–5]. In this paper previous results are updated by using the data collected during the 1998 LEP2 run, which corresponds to an integrated luminosity of 173.6 pb^{-1} at a centre-of-mass energy of 188.6 GeV. In addition slepton production in neutralino cascade decays are described for the first time in this paper.

The organization of this paper is the following. In the second section a short description of the ALEPH detector and the Monte Carlo samples used in the analyses is given. In the third section the different selections are described, starting with the search for topologies typical of the neutralino NLSP case (photons plus missing energy, non-pointing photons) followed by the topologies characteristic of the slepton NLSP scenario (acoplanar leptons, leptons with large impact parameters or detached decay vertices, stable heavy charged particles, four leptons plus missing energy). In section four a model dependent interpretation of the results in the framework of a minimal GMSB model is discussed and lower limits on the NLSP mass and on the mass scale parameter Λ are derived.

2 The ALEPH detector and Monte Carlo simulation

A detailed description of the ALEPH detector can be found in [6], and an account of its performance as well as a description of the standard analysis algorithms can be found in [7]. Only a brief overview is given here.

Charged particle tracks are measured by a silicon vertex detector (VDET), a multiwire drift chamber (ITC) and a time projection chamber (TPC). The VDET has a length of approximately 40 cm with two concentric layers of silicon wafers at average radii of 6.5 and 11.3 cm. The ITC consists of eight drift chamber layers of 2 m length between an inner radius of 16 cm and an outer radius of 26 cm. The TPC measures up to 21 space points in the radial range from 30 cm to 180 cm and has an overall length of 4.4 m. These detectors are immersed in an

axial magnetic field of 1.5 T and together achieve a transverse momentum resolution $\sigma(p_T)/p_T = 0.0006p_T \oplus 0.005$ (p_T in GeV/c). The TPC also provides up to 338 measurements of the ionisation energy loss. It is surrounded by the electromagnetic calorimeter (ECAL), which covers the angular range $|\cos\theta| < 0.98$. The ECAL is finely segmented in projective towers of approximately 0.9° by 0.9° which are read out in three segments of depth (storeys). The energy resolution is $\sigma(E)/E = 0.18/\sqrt{E} + 0.009$ (E in GeV). The iron return yoke is instrumented with streamer tubes acting as a hadron calorimeter (HCAL) and covers polar angles down to 110 mrad. Surrounding the HCAL are two additional layers of streamer tubes called muon chambers. The luminosity monitors (LCAL and SICAL) extend the calorimetric coverage down to polar angles of 34 mrad.

Using the energy flow algorithm described in [7], the measurements of the tracking detectors and the calorimeters are combined into "objects" classified as charged particles, photons, and neutral hadrons. A *good track* is defined as a charged particle track originating from the interaction region (with transverse impact parameter $|d_0| < 1$ cm and longitudinal impact parameter $|z_0| < 5$ cm), having at least four TPC hits, a transverse momentum greater than 200 MeV/c and a minimum polar angle of 18.2°. In order to get the correct charged multiplicity, photon conversions are reconstructed with a standard pair finding algorithm [7]. Electrons are identified by comparing the energy deposit in ECAL to the momentum measured in the tracking system and by using the shower profile in the electromagnetic calorimeter and the measurement of the specific ionisation energy loss in the TPC. The tagging of muons makes use of the hit patterns in HCAL and the muon chambers.

All selections are developed using Monte Carlo techniques. Monte Carlo samples corresponding to at least ten times the collected luminosity of all major background processes have been generated. For a more detailed list of the Monte Carlo generators used see [2,5]. The position of the most important cuts is determined using the $\bar{N}_{95}$ prescription [8], which corresponds to the minimisation of

the expected 95% confidence level upper limit on the number of signal events, under the hypothesis that no signal is present in the data.

3 Experimental topologies and results

The topologies expected in GMSB models are characterised by the nature and lifetime of the NLSP, as listed in Table 1. In Sect. 3.1 topologies with photons plus missing energy, expected in the χ NLSP scenario, are presented. The topologies expected in the slepton NLSP scenario are discussed in Sect. 3.2.

3.1 Topologies with photons

In the χ NLSP scenario the main signature for GMSB is the decay $\chi \to \tilde{G}\gamma$. For short neutralino lifetimes the resulting experimental signature is a pair of energetic acoplanar photons. A search for this topology is presented in Sect. 3.1.1. In Sect. 3.1.2 a new search for non-pointing single photons, designed to increase the sensitivity to long lived neutralinos, is described.

3.1.1 Short neutralino lifetimes

A search for a topology involving two acoplanar photons and missing energy has already been performed at lower centre of mass energies [2]. Events are selected with no charged tracks (except those from a conversion) and at least two photons with energies above 1 GeV inside the acceptance of $|\cos\theta| < 0.95$. Events with more than two photons are required to have at least $0.4\sqrt{s}$ of missing energy. Background from the process $e^+e^- \to \gamma\gamma(\gamma)$ is eliminated by requiring that the acoplanarity of the two most energetic photons be less than $177°$ and that there be less than 1 GeV of additional visible energy in the event. The total measured transverse momentum relative to the beam axis ($p_\perp$) is required to be greater than 3.75% of the missing energy, reducing background from radiative events, with final state particles escaping down the beam axis, to a negligible level. The energy of the least energetic photon is required to be greater than 33 GeV. This cut has been optimised assuming the MGM [9] signal model, the full integrated luminosity collected up to 188.6 GeV and that background subtraction will be performed.

No candidates are found in the data at 188.6 GeV while 1.55 events are expected from background processes. Applying this increased energy cut to the previously analysed data taken between 161 GeV and 183 GeV, one event is observed in the data while 0.74 events are expected from background processes.

The 95% CL upper limit on the production cross section at 188.6 GeV, obtained performing background subtraction and taking into account data recorded at lower energies, is in the range 0.028–0.043 pb for a 100% $\chi \to \tilde{G}\gamma$ branching ratio and χ masses in the range 45 GeV/c^2 to
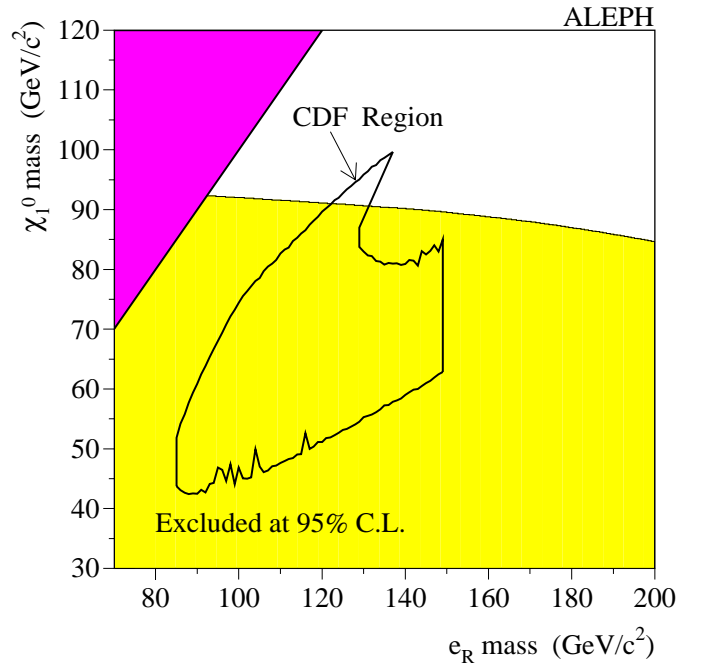
Fig. 1. The excluded region in the neutralino-selectron mass plane at 95% C.L. for a pure bino neutralino (light shaded area). Overlaid is the CDF region determined from the properties of the CDF event assuming the reaction $q\bar{q} \to \tilde{e_R}\tilde{e_R} \to ee\chi\chi \to ee\tilde{G}\tilde{G}\gamma\gamma$ [18]. The dark shaded region corresponds to a topology not covered by this analysis

94 GeV/c^2. The integrated luminosities of the lower energy data are scaled according to the cross section predictions of the MGM [9] model. The mass limit obtained for this model is $M_\chi \geq 91$ GeV/c^2 at 95% C.L. for a neutralino with lifetime smaller than 3 ns. The systematic uncertainty for this analysis is dominated by the error on the photon reconstruction efficiency, estimated to be 2.4%, and the uncertainty on the level of background from Standard Model processes, estimated to be 10% from a comparison between different Monte Carlo generators. The effect of these uncertainties on the cross section upper limit is less than 1% when taken into account by means of the method of [10]. The effect on the mass limit is negligible.

At LEP2 the production of bino-like neutralinos would proceed via t-channel selectron exchange. Right-selectron exchange dominates over left-selectron exchange. Thus, the cross section for $e^+e^- \to \chi\chi$ depends strongly on the right-selectron mass. The experimentally excluded region in the neutralino-selectron mass plane is shown in Fig. 1. Overlaid is the "CDF region", the area in the neutralino–selectron mass plane where the properties of the CDF event described in [11] are compatible with the process $q\bar{q} \to \tilde{e_R}\tilde{e_R} \to ee\chi\chi \to ee\tilde{G}\tilde{G}\gamma\gamma$. Most of the CDF region is excluded at 95% C.L. by this analysis.
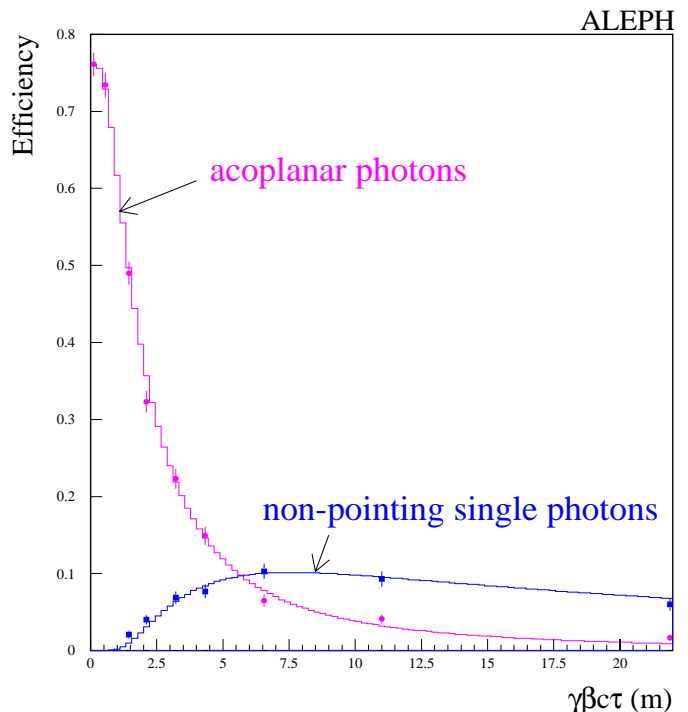
3.1.2 Longer neutralino lifetimes

In order to extend the neutralino NLSP search to longer neutralino lifetimes a dedicated analysis is developed to search for the case where one neutralino decays within the volume bounded by the ECAL, while the other decays outside the detector. This results in a topology with one visible particle, a single photon which, in general, does not originate from the interaction region. The search for this topology is based on the single photon analysis detailed in [2].

Events are selected with no tracks and exactly one photon inside the acceptance cuts of $|\cos\theta| < 0.95$ and $p_\perp > 0.0375\sqrt{s}$. To suppress background from Bhabha scattering, events are required to have no energy deposited within $14°$ of the beam axis and to have less than 1 GeV of non-photonic energy. To remove events from the process $e^+e^- \to \nu\bar{\nu}\gamma(\gamma)$ the impact parameter of the photon is required to be larger than 40 cm. This impact parameter is defined to be the minimum of the three possible values calculated from the pairings of the barycentres of the photon shower measured in each of the three ECAL segments.

Cosmic ray events that traverse the detector are primarily eliminated by the charged track veto or by hits recorded in the outer part of the HCAL. Residual cosmic ray events are rejected by requiring that at least 90% of the photon's energy be recorded in the ECAL. Background muons, produced by the interaction of the LEP beams with matter, cross the detector with a trajectory essentially parallel to the beam axis. They are eliminated by requiring that there be no activity in either the muon chambers or the ECAL within a transverse distance of 15 cm of the photon candidate. Events with detector noise in the ECAL are removed by requiring that there be no more than 50 fired storeys, in addition to those associated with the photon, in any module. Finally, the interaction time of the event is required to be within 40 ns of a beam crossing.

The efficiency of this selection depends on the neutralino's laboratory decay length and has a maximum value of 10% for decay lengths around 8 m. The dependence of the efficiency on the neutralino lifetime has been checked on fully reconstructed Monte Carlo signal samples for decay lengths up to 200 m. The residual background from the $e^+e^- \to \nu\bar{\nu}\gamma(\gamma)$ process is estimated to be 0.4 events in the combined 161–188.6 GeV data sample. This estimate takes into account the number of events before the pointing cut (the cut on the photon impact parameter) and the probability for photons from the interaction region to pass the pointing cut as estimated from a sample of $e^+e^- \to \gamma\gamma(\gamma)$ data. The remaining contribution from cosmics, beam muons and detector noise is estimated from the number of events which pass all cuts except the final cut on the interaction time of the event and is less than 0.4 events at 95% C.L. When the selection is run on the data no events are selected allowing an upper limit on the production cross section to be derived.

The efficiencies of the two analyses described in this section are shown as a function of neutralino lifetime in

Fig. 2. Selection efficiency as a function of the neutralino lifetime for the two analyses described in Sect. 3. The points are the efficiencies obtained from fully simulated Monte Carlo samples while the histograms represent the parameterizations used in the computation of the limits

Fig. 2. The non-pointing photon analysis allows the exclusion of χ masses as high as 55 GeV/c^2 for $c\tau_\chi$ values smaller than 100 m, assuming the MGM model described in [9].

3.2 Topologies with leptons

In the case of a slepton NLSP, the pair-production process $e^+e^- \to \tilde{\ell}\tilde{\ell} \to \ell\tilde{G}\ell\tilde{G}$ is expected to be one of the main experimental signatures. The signal final state topology depends strongly on the slepton lifetime. Four different analyses are performed, each corresponding to a specific range of mean decay length. The search for acoplanar leptons covers the case of very small lifetimes, the searches for tracks with large impact parameter and for kinks are used in the intermediate range, whereas for very large lifetimes a search for heavy stable charged particles is performed.

In region of the GMSB parameter space where the mass difference between the lightest neutralino and the sleptons is small, the cascade decay $e^+e^- \to \chi\chi \to \tilde{\ell}\ell\tilde{\ell}\ell \to \ell\ell\tilde{G}\ell\ell\tilde{G}$ can compete with the direct slepton production and can increase the sensitivity to GMSB signatures. This process benefits from a large cross section; the χ is expected to be mainly bino and the right-selectron is expected to be light. It also benefits from a clear experimental signature: four leptons are produced in the final state (two of them could be soft depending on the χ-$\tilde{\ell}$ mass dif-

ference) and in half of the cases the two most energetic leptons have the same charge (χ are Majorana particles).

Searches for direct slepton production have already been performed at centre-of-mass energies up to 184 GeV [3–5]. They are partially reoptimized here to account for the increased centre-of-mass energy and the higher luminosity. Therefore only a short outline of the general concepts is given in the following subsections, omitting details of the selection criteria where they have been left unchanged with respect to [3–5].

3.2.1 Short-lived sleptons

If the slepton lifetime is negligible ($c\tau_{\tilde{\ell}} << \ell_{detector}$) GMSB signatures do not differ from those in models with gravity mediated SUSY breaking (in the region of the parameter space where the χ LSP has a small mass). The searches for acoplanar leptons described in [4,5] and updated for the 188.6 data in [12] are therefore used in the very small lifetime domain. In the 188.6 GeV data sample a total of 33, 28 and 21 events are selected by the acoplanar electrons, acoplanar muons and acoplanar taus analyses. This has to be compared with 32.8, 29.6 and 15.5 background events expected for these three topologies form SM processes.

3.2.2 Medium-lived sleptons

For both the large impact parameter and the kink searches, a common preselection against background from $\gamma\gamma$ events is applied, requiring a minimum visible mass of $0.03\sqrt{s}$ and at least one well measured track with high transverse momentum. Dilepton and Bhabha events are suppressed by an upper cut on the visible energy of $0.9\sqrt{s}$ for the kink search and of $0.65\sqrt{s}$ for large impact parameter search. Tracks identified as coming from photon conversions are removed from the event.

The rejection of events containing cosmic muons is improved with respect to [5]. Cosmic muons are often reconstructed as two different tracks, possibly shifted along the direction of the beam axis, due to their time offset with respect to the nominal beam crossing. Such tracks are identified by refitting the TPC hits of the two parts under the hypothesis of a single helix, taking into account the possible shift along the z axis where necessary.

The procedure used to reconstruct kinks is described in [5] and has not been modified. As described there, real decay signals are separated from kinks caused by hard bremsstrahlung and hadronic interactions using the kink angle and an energy veto in the inner track direction. To account for the higher luminosity the cut on the momentum of the outer track is increased from $0.01\sqrt{s}$ to $0.015\sqrt{s}$.

The large impact parameter selection requires at least one track with an impact parameter of more than 1 cm (track 1) and a minimum momentum of $0.01\sqrt{s}$. The number of additional tracks with TPC hits is restricted to one or three. In the latter case the three tracks must be consistent with a three-prong tau decay. Such track triplets are considered in the following as one track (track 2) with a momentum given by the sum of the momenta of the triplet. For these triplets the impact parameter is defined as the average of the impact parameters of the three tracks. The acoplanarity and the acollinearity of track 1 and track 2 are used to suppress dilepton and $\gamma\gamma$ background. In addition the impact parameter of track 2 is required to be in excess of 0.025 cm.

With the luminosity collected at 188.6 GeV a background of 0.5 events from tau pairs and Bhabha events is expected in the kink search. The expected background of 0.1 events in the large impact parameter search is dominated by Bhabha events. For each of the two selections a background of 0.3 events is estimated from cosmic muons.

In the data no candidate events are selected by the large impact parameter analysis and one candidate is selected by the kink analysis. This candidate is consistent with a three-prong tau decay.

3.2.3 Long-lived sleptons

When the slepton lifetime becomes much larger than the detector size the sleptons behave as heavy charged particles. They can be identified by using the characteristic kinematics of their pair production and the high specific ionization that they are expected to release in the TPC. The same selection criteria as in [3] are used here. A total Standard Model background of about 0.9 events is expected, half of it coming from double-radiative dimuon events and half from ditau events. In the data, three events are selected by the more kinematics-oriented analysis (defined as medium-mass in [3]) while no events are selected by the analysis based mainly on the reconstruction of highly ionizing pairs (referred to as high-mass in [3]). If the three candidates were interpreted as pair-produced heavy particles, their measured masses would be (54.3 ±1.4) GeV/c^2, (61.4±1.3) GeV/c^2 and (60.5±1.4)GeV/c^2.

The systematic uncertainty on the selection cuts based on kinematics is studied with a dimuon sample, selected with criteria independent of those used in the analysis, on which the performance of the tracking system is checked. The dE/dx performance is checked with electrons, pions and muons, selected by using the information from the calorimeters, over a large β range. A total systematic error of less than 5% on the selection efficiency is estimated. As the number of candidates is consistent with the expected background, a 95% C.L. upper limit on the production cross section of the stable sleptons is derived; it corresponds to about 30 fb for slepton masses in the range 65–90 GeV/c^2.

By combining all the direct slepton analyses described above and including the results obtained at lower centre-of-mass energies [3–5], it is possible to derive a limit on the slepton mass as a function of the slepton lifetime. This is shown in Fig. 3 for the stau NLSP scenario. A 95% C.L. lower limit of 68 GeV/c^2 can be derived on the $\tilde{\tau}_R$ mass and of 85 GeV/c^2 on the degenerate co-NLSP $\tilde{\ell}_R$ mass.
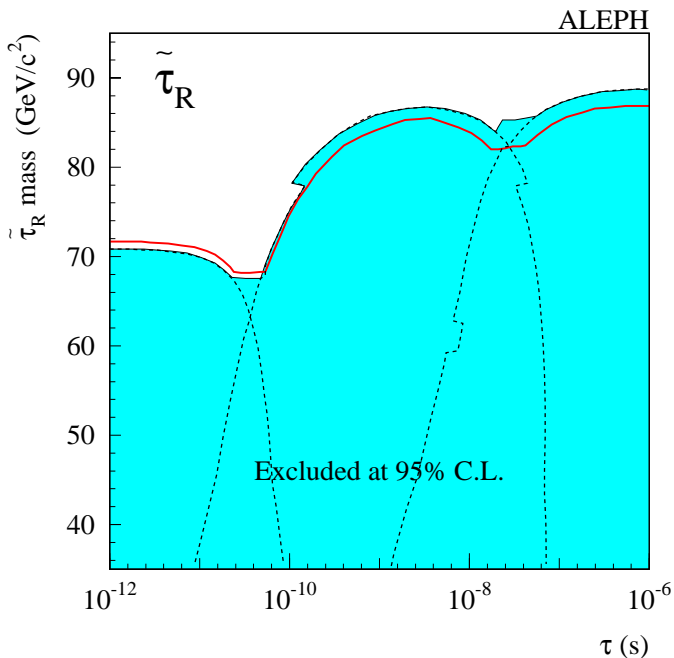
Fig. 3. Excluded stau-right mass at 95% C.L. as a function of its lifetime. The thick curve gives the expected limit. The dashed curves show the exclusions provided by the different analyses described in the text

The limit on the co-NLSP $\tilde{\ell}_R$ is evaluated by taking into account only the s-channel for $\tilde{e}$ production.

3.2.4 Neutralino to slepton cascade topologies

In this section, searches for the cascade process $e^+e^- \to \chi\chi \to \tilde{\ell}\ell\tilde{\ell}\ell \to \ell\ell\tilde{G}\ell\ell\tilde{G}$ are described. The slepton lifetime is assumed to be negligible. The final state can have different lepton flavour composition depending on which particle is the NLSP. If the stau is much lighter than the other sleptons (typical case of the large $\tan\beta$ scenario) four taus are produced. If the three sleptons are degenerate in mass the final state will consist of two pairs of same-flavour leptons in about $1/3$ of the cases and of two pairs of mixed-flavour leptons in about $2/3$ of the cases. In order to cover these different scenarios, selections for all possible topologies ($\tilde{\mu}\tilde{\mu}$, $\tilde{e}\tilde{e}$, $\tilde{\tau}\tilde{\tau}$, $\tilde{\mu}\tilde{\tau}$, $\tilde{e}\tilde{\tau}$ and $\tilde{\mu}\tilde{e}$) are developed. These selections are based on the same variables as those described in [5]. In particular the lepton identification (electron, muon and tau) is the same. Here only the main aspects of the selections are summarised. The details of the selections are given in the appendix A.

All the topologies have a common anti-$\gamma\gamma$ preselection almost identical to that adopted in [5]. This is based on the rejection of events with low transverse momentum or with energy deposits at small polar angles which indicate the presence of a scattered electron. A small charged track multiplicity is also required in order to reject $q\bar{q}(\gamma)$ events and hadronic WW and ZZ decays. For each topology, at least two energetic leptons are required, where a lepton can also be a jet with small multiplicity and invariant

Table 2. Selection efficiencies, expected Standard Model background and selected candidates for the various slepton cascade topologies. The background is normalised to an integrated luminosity of 173.6 pb^{-1}

Channel	Efficiency (%)	Background	Data candidates
$\tilde{\mu}\tilde{\mu}$	75	0.1	1
$\tilde{e}\tilde{e}$	65	0.5	1
$\tilde{\tau}\tilde{\tau}$	55	5.1	4
$\tilde{\mu}\tilde{\tau}$	60	1.0	0
$\tilde{e}\tilde{\tau}$	60	1.2	2
$\tilde{e}\tilde{\mu}$	65	0.6	1

mass, in order to select hadronic tau decays. They must be acoplanar, acollinear and their energies must be in the range allowed by the signal kinematic properties. These cuts reject most of the $\ell\bar{\ell}(\gamma)$ background. The kinematic cuts are also effective against WW and Weν backgrounds where the W decays leptonically. Since two other leptons (soft for small χ-$\tilde{\ell}$ mass difference) are expected in the signal topology at least one additional lepton is required in the selection. If the charges of the two most energetic leptons are not equal, the acoplanarity and the kinematic cuts are tightened.

The performance of the different analyses is listed in Table 2. The efficiencies refer to a mass difference between the neutralino and the slepton of $5\,\mathrm{GeV}/c^2$ and to a neutralino mass of $90\,\mathrm{GeV}/c^2$. The energy spectra of the most and of the second most energetic lepton for the different topologies, after some preselection cuts, are shown in Fig. 4.

The systematic uncertainty on the selection efficiency is studied by checking the main selection variables (lepton identification and isolation, acoplanarity, acollinearity, etc.) on leptonic samples selected from the data. A total systematic uncertainty of 2% is evaluated for all the variables related to the lepton identification. It is found that in about 8% of the random triggers there is an energy deposit within the $12°$ cone around the beam line. The selection efficiency is reduced by this amount. The systematics uncertainty on the background is estimated to be 2% dominated by the uncertainty on the lepton identification.

The neutralino to slepton cascade analyses are applied to the data collected at 188.6 GeV and the number of selected candidates is reported in Table 2. No excess is observed, hence limits on the production cross section for the different topologies are derived. The limits are between 30 and 90 fb, where the worst limit is obtained for the $\tilde{\tau}\tilde{\tau}$ topology. In the evaluation of the limits the background has been subtracted in the basis of method [10].

These cross section upper limits can be translated into exclusions in the neutralino-slepton mass plane, as shown in Sect. 4, once some model dependent assumptions are made.
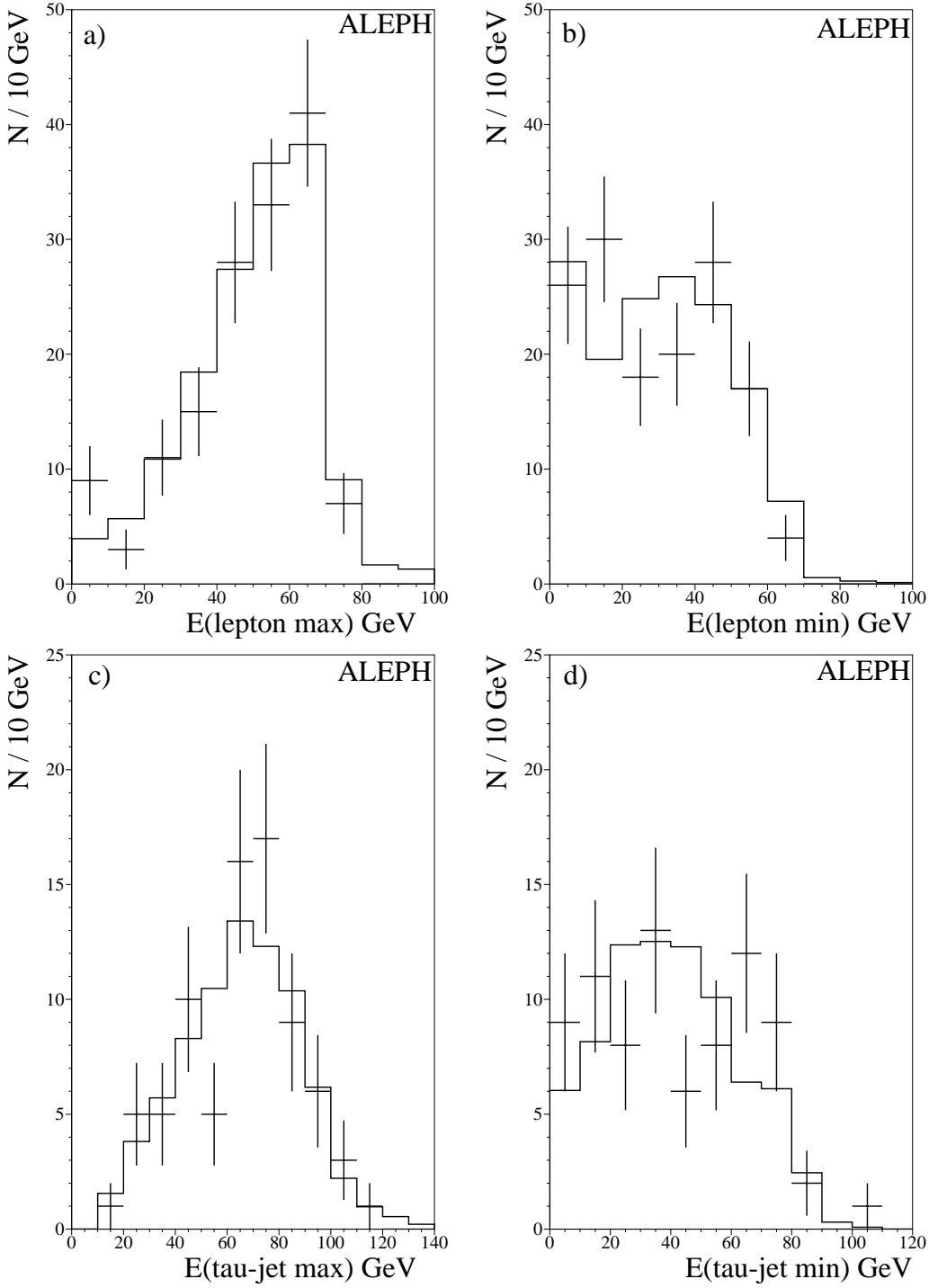
Fig. 4a–d. The energy spectra for the most and the second most energetic lepton are shown in Figs. **a** and **b** for the $\tilde{e}\tilde{e}$, $\tilde{e}\tilde{\mu}$ and $\tilde{\mu}\tilde{\mu}$ topologies after preselection cuts. The same distributions for the $\tilde{\tau}\tilde{\tau}$, $\tilde{\tau}\tilde{\mu}$ and $\tilde{\tau}\tilde{e}$ topologies are shown in Figs. **c** and **d**. The histograms represent the Monte Carlo SM background while the points are the data

The search for the cascade decay $\chi \rightarrow \tilde{\tau}\tau \rightarrow \tau\tau\tilde{G}$ allows the extension of the $\tilde{\tau}$ mass lower limit, in the $\tilde{\tau}$ NLSP scenario, up to 84 $\mathrm{G}eV/c^2$ if the χ is lighter than 87 $\mathrm{G}eV/c^2$, the χ-$\tilde{\tau}$ mass difference is greater than the τ mass, and the $\tilde{\tau}$ lifetime is negligible. The χ field composition is assumed to be 100% bino and the right-selectron mass is assumed to be 1.2 times the neutralino one.

4 Interpretation of the results in the minimal GMSB model

A scan over the parameter space of a minimal GMSB model is performed. This model is defined by the following set of parameters: Λ, the universal mass scale of SUSY particles; N5, the number of messenger pairs; M_{mess}, the messenger mass scale; $\tan\beta$, the ratio between the vacuum expectation values of the two Higgs doublets; $\mathrm{sign}(\mu)$, where μ is the higgsino mass parameter; and $\sqrt{\mathrm{F}}$, the

Table 3. Ranges used in the GMSB parameter scan

Parameter	Lower limit	Upper limit
M_{mess}	10^4 GeV	10^{12} GeV
$M_{\tilde{G}}$	10^{-10} GeV	10^{-4} GeV
Λ	10^3 GeV	$\min(\sqrt{F}, M_{mess})$
$\tan\beta$	1.3	38
N5	1	5
$\text{sign}(\mu)$	$-$	$+$

Fig. 5. Region excluded at 95 % confidence level in the $log_{10}(c\tau_\chi)$-M_χ plane for negative μ, N5 $=$ 1, $M_{mess} =$ 10^{12} GeV$/c^2$ and $\tan\beta = 20$. The horizontal-dashed region is excluded by the searches for acoplanar-photons and single photon. The crossed region is excluded by the MSSM acoplanar-lepton searches. The vertical-dashed region is excluded by the MSSM chargino searches

SUSY breaking scale (which is related to the gravitino mass by the formula given at the end of this section). As in SUGRA models the absolute value of μ is obtained by imposing dynamical electroweak symmetry breaking. The aim of this scan is to understand which topologies contribute to exclude regions in the parameter space, to set a lower limit on the NLSP mass and on the universal mass scale Λ.
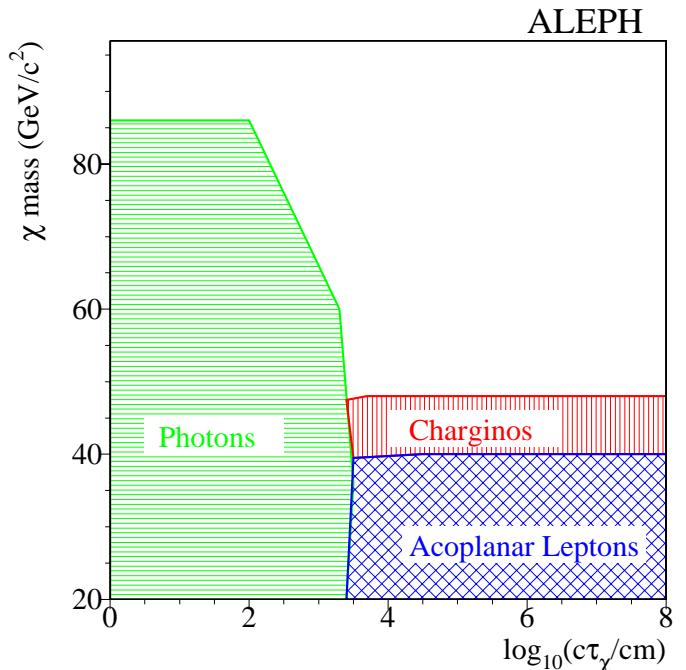
In addition to the analyses described in this paper, results obtained at LEP1 [13,14] are also used to exclude very low NLSP masses. The searches for the charginos [15] and sleptons [12] of the minimal supersymmetric extension of the SM (MSSM) up to 189 GeV are used in this scan to obtain indirect constraints on the χ NLSP mass, when the neutralino lifetime is very long.

The scan is performed in the ranges specified in Table 3. The granularity of the scan is such that more than 10^7 points in the GMSB parameter space are tested. Points where the NLSP mass is higher than the beam energy (94.3 GeV) are not considered (i.e., not excluded). This scan is not exhaustive, but it covers a large portion of the allowed range of the minimal GMSB parameter space. The implication of possible extensions of the scan ranges is discussed at the end of this section. For each point of the scan, SUSY particle masses, cross sections, branching ratios and lifetimes are evaluated by using an interface to the ISAJET [16] program. All these properties are taken into account when the possible exclusion of the scanned point by the ALEPH searches is evaluated. A point in the minimal GMSB parameter space is considered as excluded if the most sensitive of the accessible topologies is excluded at 95 % confidence level.

4.1 Lower limit on the NLSP mass

In the stau NLSP scenario the 95% CL lower limit on $M_{\tilde{\tau}}$ is almost unaffected by the stau mixing and is 67 GeV$/c^2$ for any stau lifetime, over the full scan range.

The validity of the limits obtained in the χ NLSP scenario over the parameter space covered by the scan is studied. For short χ lifetimes ($c\tau_{NLSP} << \ell_{detector}$) the limit on the χ mass is lowered by about 5 GeV$/c^2$ (from 91 to 86 GeV$/c^2$) with respect to the value reported in Sect. 3.1, where the more restrictive model [9] is assumed. For long χ NLSP lifetimes ($c\tau_{NLSP} >> \ell_{detector}$) the neutralino becomes invisible and only indirect exclusions are possible,

similarly to what happens in the SUGRA LSP determination [15]. The relationship between the χ mass and the $\tilde{\ell}$ and $\tilde{\chi}^\pm$ masses can be exploited to put indirect limits on the χ mass using the ALEPH results of the MSSM slepton [12] and chargino [15] searches. An example is shown in Fig. 5, where the contribution of the MSSM slepton and chargino searches to the χ NLSP exclusion is illustrated in the M_χ-$c\tau_{NLSP}$ plane (for $M_{mess} = 10^{12}$ GeV$/c^2$, $\tan\beta = 20$, N5 $=$ 1 and negative μ) together with the exclusion given by acoplanar photons and single-photon topologies. A general scan gives a lower limit on M_χ of 45 GeV$/c^2$ for any NLSP lifetime (i.e., for any gravitino mass). This is also the absolute lower limit on the NLSP mass obtained in this scan.

The interplay between the different searches for short NLSP lifetimes in the M_χ-$M_{\tilde{\tau}}$ plane is shown in Fig. 6a. It can be seen that all three analyses (acoplanar γ's, acoplanar τ's and multi leptons) contribute to exclude some points in this plane. The same plane for long NLSP lifetimes is shown in Fig. 6b. The absolute lower limit on the NLSP quoted above is visible in this plot.

4.2 Lower limit on Λ

In the context of this minimal GMSB model, it is relevant to put a lower limit on the parameter Λ which fixes the universal mass scale of the SUSY particles. A lower
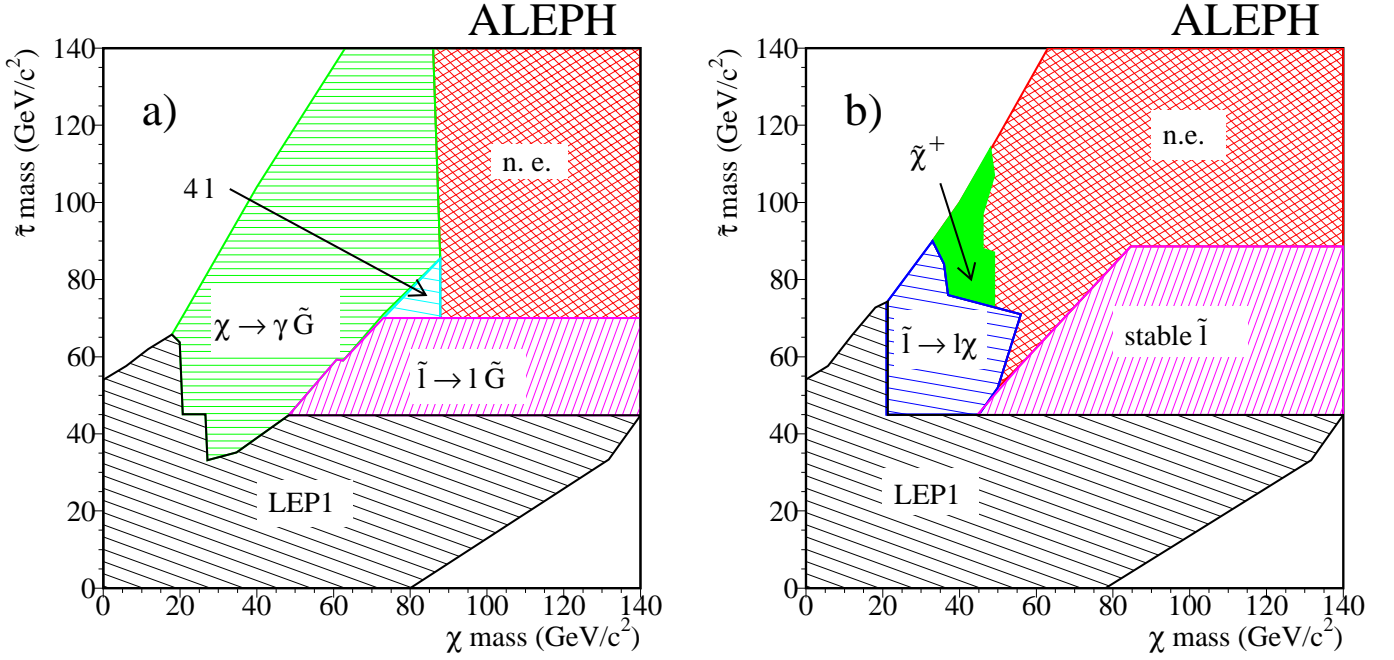
Fig. 6a,b. Region excluded at 95 % confidence level in the M_χ-$M_{\tilde{\tau}}$ plane for short **a** and long **b** NLSP lifetimes by the different analyses described in the text. The crossed region corresponds to point not excluded in the scan. In the scan no points have been found in the white region
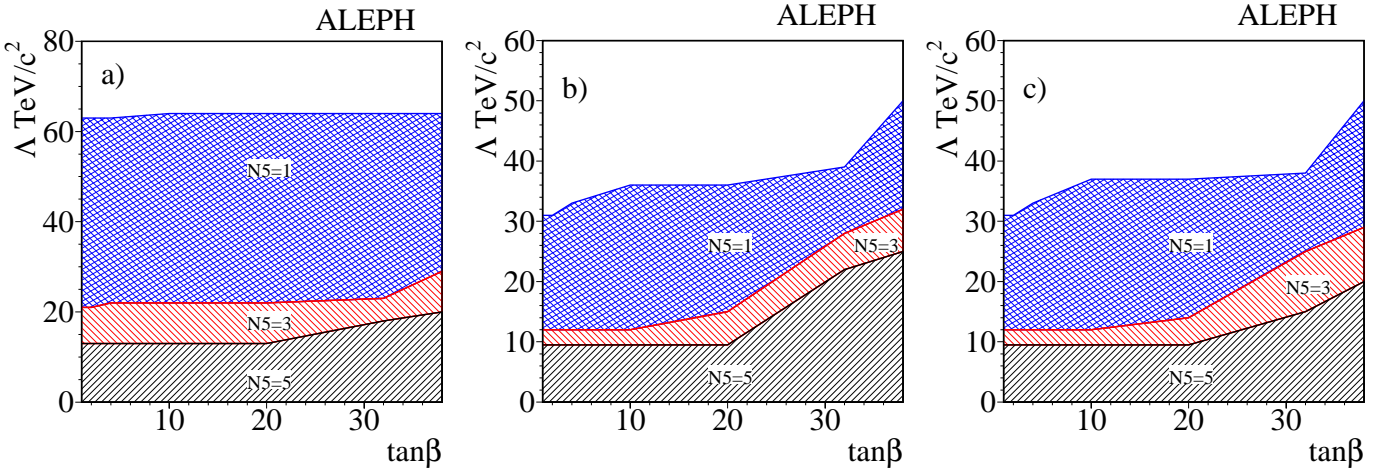

Fig. 7a–c. Region excluded at 95 % confidence level in the Λ-$\tan\beta$ plane for **a** short, **b** long and **c** any NLSP lifetimes

limit on the NLSP mass implies a lower limit on this parameter. The relation between the SUSY particle masses and Λ depends on N5, therefore it is interesting to provide this limit as a function of N5. The excluded region for the parameter Λ as a function of $\tan\beta$ is shown in Fig. 7, for different N5 and different NLSP lifetimes. In the "short-NLSP-lifetime" scenario the lower limit on Λ is about 12 TeV. In the "long-NLSP-lifetime" scenario the lower limit on Λ is about 9 TeV and corresponds to the absolute lower limit on Λ obtained in the full scan. This limit occurs for N5 = 5, $M_{mess} = 10^{12}\,\mathrm{GeV}/c^2$, $\tan\beta$ in the range 1.5–20 and a large gravitino mass (stable NLSP). For values of $\tan\beta$ larger than 20 the stau becomes the NLSP and the lower limit on Λ is improved thanks to the search for long-lived staus. At this point the χ is the NLSP

and has a mass of about 60 GeV/c^2; the next-to-NLSP is the $\tilde{\tau}$ with a mass of about 72 GeV/c^2 and the MSSM stau searches are not able to exclude this point. All other SUSY particles are above threshold. The lower limit on Λ as a function of N5 (for any lifetime) is shown in Fig. 8a. The final result of the scan is that the limit $\Lambda > 9$ TeV can be derived.

It should be stressed that the range of parameter space over which this limit holds is reasonably large but not exhaustive. An increase in the $\tan\beta$ scan range would not change this result, because for values of $\tan\beta$ larger than 38 the $\tilde{\tau}_1$ mass becomes lower. The only parameters that can invalidate the lower limit on Λ are N5 and M_{mess}. For larger values of N5 or M_{mess}, the χ and the $\tilde{\ell}$ masses are outside the LEP2 reach for quite modest values of Λ. As

ALEPH   ## ALEPH
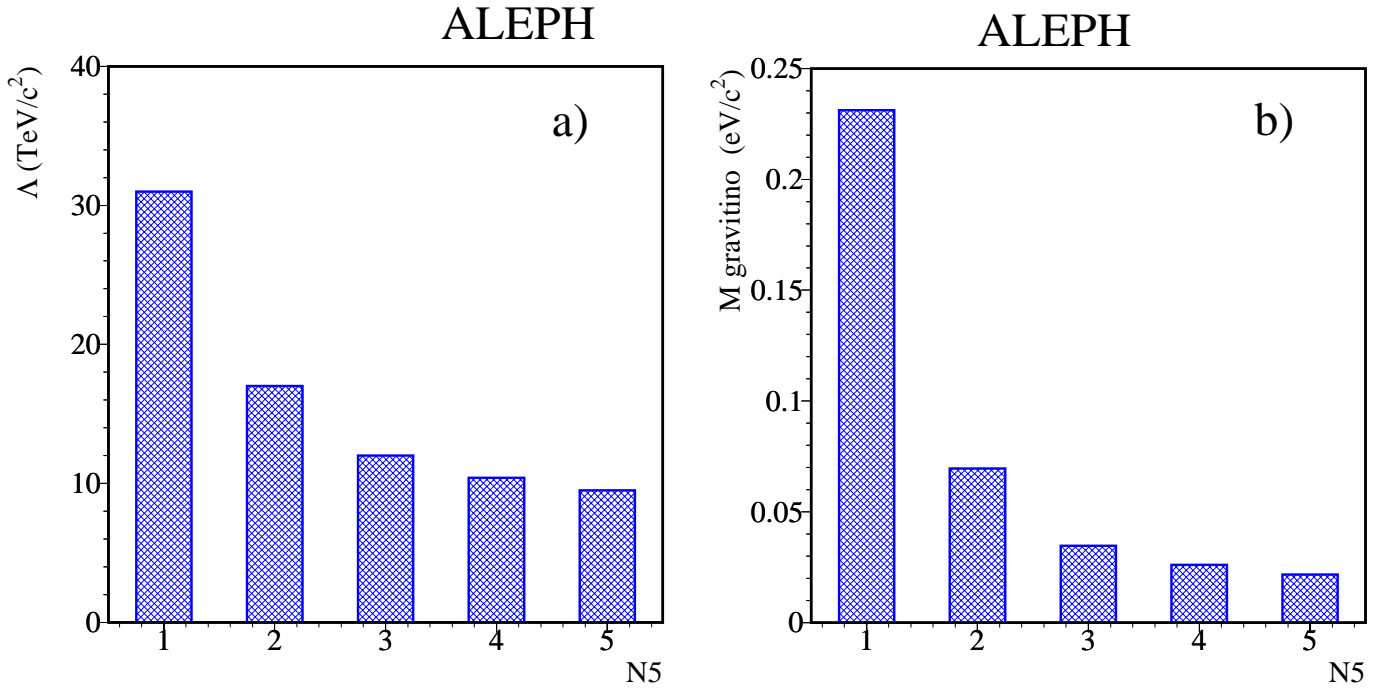
Fig. 8a,b. Exclusions at 95 % confidence level **a** for Λ and **b** for $M_{\tilde{G}}$ as a function of N5, derived from the minimal GMSB scan

an example it has been observed (with a dedicated scan) that for values of N5 = 6 and $M_{mess} = 10^{14}$ GeV the lower limit on Λ goes down to about 5 TeV.

In this scan the MSSM Higgs exclusions reported in [17] are not used. In the minimal GMSB model, the stop mixing is expected to be small so the ALEPH Higgs limits would exclude the region with $1 \leq \tan\beta \leq 2$. This would, however, only have a small impact on both the NLSP and on the Λ limits presented here.

It is worth mentioning that the lower limit on Λ provides an indirect constraint on $\sqrt{F}$ and therefore on the gravitino mass. In fact in GMSB models the relation $\Lambda \leq \sqrt{F}$ is satisfied (this relation is based on the simple assumption of positive messenger masses-squared, as can be easily derived from [1]). By using this relation and the equation

$$M_{\tilde{G}} = \frac{F}{\sqrt{3}M'_P}$$

(where $M'_P = 2.4 \times 10^{18}$ GeV/c^2 is the reduced Planck mass) an indirect lower limit on $M_{\tilde{G}}$ as a function of N5 is derived, as shown in Fig. 8b. The lower limit on $\sqrt{F}$ of about 9 TeV implies a lower limit on $M_{\tilde{G}}$ of 2×10^{-2} eV/c^2.

5 Conclusions

A large variety of GMSB topologies have been searched for in the 188.6 GeV ALEPH data sample. No evidence for new physics is found. In the χ NLSP scenario a lower limit of 91 GeV/c^2 on the NLSP mass is derived at 95 % C.L., assuming the MGM model, described in [9], and a short χ lifetime. Assuming the same model [9] but for

Table 4. Selection cuts for the different topologies described in Sect. 3.2.4. The cuts with the * are applied only to the events in which the two most energetic leptons have opposite charge

Variable	$\tilde{\mu}\tilde{\mu}$	$\tilde{e}\tilde{e}$	$\tilde{e}\tilde{\mu}$
M_{tot}(GeV)	>4	>5*	>4*
N_{ch}	=(2,3,4)	=(2,3,4)	=(2,3,4)
N_ℓ	$\geq$3	$\geq$3	$\geq$3
$E_{12}/\sqrt{s}$	<0.05	=0*	<0.05*
AcopT	<175	<175	<175
$E_{30}/\sqrt{s}$	<0.086	<0.086	<0.086

longer χ lifetime, the non-pointing photon analysis allows the exclusion of χ masses as high as 55 GeV/c^2 for $c\tau_\chi$ values smaller than 100 m.

In the stau NLSP scenario $\tilde{\tau}$ masses lower than 67 GeV/c^2 are excluded at 95 % C.L., for any values of the stau lifetime. In the slepton co-NLSP scenario the lower limit on the slepton mass extends up to 85 GeV/c^2 (only s-channel production for the right-selectron is assumed) for any slepton lifetime. The search for the cascade decay $\chi \rightarrow \tilde{\tau}\tau \rightarrow \tau\tau\tilde{G}$ allows the extension of the $\tilde{\tau}$ mass lower limit, in the $\tilde{\tau}$ NLSP scenario, up to 84 GeV/c^2 if the χ is lighter than 87 GeV/c^2, the χ-$\tilde{\tau}$ mass difference is greater than the τ mass, and the $\tilde{\tau}$ lifetime is negligible. The χ field composition is assumed to be 100% bino and the right-selectron mass is assumed to be 1.2 times the neutralino one.

A scan over the parameters of a minimal GMSB model is performed in order to check the sensitivity of the ALEPH

Table 5. Selection cuts applied to the $\tilde{\mu}\tilde{\mu}$, $\tilde{e}\tilde{e}$ and $\tilde{e}\tilde{\mu}$ topologies, described in Sect. 3.2.4, in case the two most energetic leptons have different charge

Variable	$\tilde{\mu}\tilde{\mu}$	$\tilde{e}\tilde{e}$	$\tilde{e}\tilde{\mu}$
$E_{\ell-MAX}$(GeV)	>8 AND < 85	>9 AND <80	>17 AND <75
$E_{\ell-min}$(GeV)	>2 AND < 65	>3.2 AND <60	-
$E_{\gamma iso}$(GeV)	-	=0	-
E_{lt}(GeV)	-	-	>28 AND <60
Acop	<171	<171	<172

Table 6. Selection cuts for the $\tilde{\tau}\tilde{\tau}$ topology described in Sect. 3.2.4. The first three cuts are applied to all the events while only the second OR the third series of cuts must be satisfied by the event

Variable	$\tilde{\tau}\tilde{\tau}$
Applied to all events	
M_{tot}(GeV/c^2)	>4
$E_{12}/\sqrt{s}$	< 0.05
N_{τ}	≥ 3
alternative 1	
N_{ch}	=(3,4,5,6,7)
Thrust	< 0.95
Acol	<170
Acop	<169
$M_{\tau\tau}$(GeV/c^2)	< 78
M_{miss}(GeV/c^2)	> 40
$N_{ch\tau 1}$	>0
$N_{ch\tau 2}$	>0
$p_{\tau 1}$(GeV/c)	<40
$p_{\tau 2}$(GeV/c)	<15
alternative 2	
$|\text{Charge}(\tau_1 + \tau_2)|$	≤ 2
N_{ch}	=(4,5,6,7)
Acol	<174
Acop	<174
Thrust	< 0.98
$M_{\tau\tau}$(GeV/c^2)	< 100

Table 7. Selection cuts for the $\tilde{\mu}\tilde{\tau}$ and $\tilde{e}\tilde{\tau}$ topologies described in Sect. 3.2.4

Variable	$\tilde{\mu}\tilde{\tau}$	$\tilde{e}\tilde{\tau}$
M_{tot}(GeV/c^2)	>4	>4
$E_{12}/\sqrt{s}$	<0.05	< 0.05
N_{ch}	=(4,5,6)	=(4,5,6)
N_{τ}	≥ 1	≥ 1
$E_{\tau-MAX}$(GeV)	>21 AND <73	>21 AND <73
$E_{\tau-min}$(GeV)	<58	<58
$N_{\ell=\mu ore}$	≥ 1	≥ 1
$E_{\ell-min}$ (GeV)	>0 AND <26	>0 AND <25
Thrust	<0.97	<0.97
NH_{τ}	< 2	<2
$M(E-\tau)$(GeV/c^2)	< 85	<85
M_{miss}(GeV/c^2)	>38	>38 AND <170
Acol	< 175	<175

universal SUSY mass scale Λ and an indirect lower limit of 2×10^{-2} eV/c^2 on the gravitino mass.

Appendix $\chi \to \tilde{\ell}\ell \to \ell\ell\tilde{G}$ selection cuts

In this appendix the cuts used by the cascade slepton analyses, described in Sect. 3.2.4, are given in detail. The variables used are the same as those defined in the previously published slepton paper [5].

results to the assumptions made in deriving exclusions and to show the interplay of the different analyses in covering the accessible GMSB parameter space. This scan provides a lower limit of 45 GeV/c^2 on the NLSP mass (for any NLSP lifetime), a lower limit of 9 TeV on the

Anti-$\gamma\gamma$ preselection

The following anti-$\gamma\gamma$ preselection cuts applied to all the four-lepton analyses:

- $p_\perp/\sqrt{s} > 0.05$ or $((\mid \phi_{\mathrm{miss}} - 90 \mid = 15$ or $\mid \phi_{\mathrm{miss}} - 270 \mid = 15)$ and $p_\perp/\sqrt{s} > 0.075)$
- $\theta_{\mathrm{diff}} > 5°$ or $\theta_{scatt} > 15°$
- $\mathrm{E}_{nh}/\mathrm{E}_{tot} < 0.30$ or ($\mathrm{E}_{nh}/\mathrm{E}_{tot} < 0.45$ and $p_{\perp\mathrm{nnh}}/\sqrt{s} > 0.03$)
- $\mid \cos\theta_{\mathrm{miss}} \mid < 0.95$

The cut variables are defined as follows: $p_\perp$ is the transverse momentum of the event, $\sqrt{s}$ is the centre-of-mass energy, ϕ_{miss} is the azimutal direction of the missing momentum, θ_{diff} and θ_{scatt} are two variables associated to the $\gamma\gamma$ kinematic hypothesis, E_{nh} is the reconstructed neutral-hadron energy, E_{tot} is the total energy of the event, $p_{\perp\mathrm{nnh}}$ is the transverse momentum of the event evaluated without the neutral hadrons and θ_{miss} is the polar angle of the missing momentum.

$\tilde{e}\tilde{e}$, $\tilde{\mu}\tilde{\mu}$ and $\tilde{e}\tilde{\mu}$ selections

The same muon and electron identification as described in the MSSM scalar paper [5] is applied here. After the preselection the cuts listed in Table 4 are applied to the three topologies that do not involve taus in the final state.

After these cuts the charge of the two most energetic leptons is checked. If the two most energetic leptons have equal charges, no further selection is needed (except for the $\tilde{e}\tilde{e}$ selection, in which the energy of the most energetic lepton is required to be smaller than 90 GeV) because the Standard Model background is reduced to a very low level. Otherwise the selection criteria listed in Table 5 are applied.

The variables listed in the tables are defined as follows: M_{tot} is the invariant mass of the event, N_{ch} is the number of tracks and N_ℓ is the number of identified leptons. In the $\tilde{e}\tilde{e}$ selection at least three electrons and in the $\tilde{\mu}\tilde{\mu}$ selection at least three muons are required. In the $\tilde{e}\tilde{\mu}$ selection one of the two most energetic track must be identified as an electron and the other as a muon. Furthermore not more than two leptons of the same type are accepted. The E_{12} variable is the total energy reconstructed in a $12°$ cone around the beam line, AcopT is the transverse acoplanarity of the two most energetic leptons, E_{30} is the total energy reconstructed in a $30°$ cone around the beam line, $\mathrm{E}_{\ell-MAX \ (min)}$ is the energy of the first (second) most energetic lepton in the event. $\mathrm{E}_{\gamma\mathrm{iso}}$ is the total energy of isolated photons, E_{lt} the energy of the most energetic track and Acop is the angle between the two most energetic leptons in space.

$\tilde{\tau}\tilde{\tau}$, $\tilde{\mu}\tilde{\tau}$ and $\tilde{e}\tilde{\tau}$ selections

After the preselection further selection cuts are applied. The cuts for the $\tilde{\tau}\tilde{\tau}$ topology are described in Table 6 while

the cuts for mixed topologies involving one $\tilde{\tau}$ are listed in Table 7.

For the $\tilde{\tau}\tilde{\tau}$ selection the event must contain at least three jets (JADE algorithm with $y_{cut} = 0.001$) with an invariant mass smaller than $6\,\mathrm{GeV}/c^2$. Subsequently the two most energetic jets with a mass smaller than $2\,\mathrm{GeV}/c^2$ and either one or three charged tracks are considered (as jet 1 and 2). The definition of the reconstructed tau is given in the slepton paper [5].

The definition of the variables used in Tables 6 and 7 are the following: Acol is the acollinearity of the two most energetic taus, Acop is their acoplanarity, $\mathrm{M}_{\tau\tau}$ is the invariant mass of the two most energetic taus, M_{miss} is the missing mass of the event, $\mathrm{N}_{ch\tau1,2}$ is the number of charged tracks in the two most energetic tau jets, $p_{\tau1,2}$ is the momentum of jet 1 or 2, $\mid \mathrm{Charge}(\tau_1 + \tau_2) \mid$ is the sum of the reconstructed charges of the tracks in jets 1 and 2, $\mathrm{E}_{\tau-MAX}$ (min) is the energy of the first (second) most energetic tau of the event, NH_τ is the number of neutral hadrons reconstructed in the tau jet and $\mathrm{M}(\mathrm{E}\text{-}\tau)$ is the invariant mass of the event once the most energetic tau jet has been removed.

References

1. For a review see: G.F. Giudice, R. Rattazzi, Theories with Gauge–Mediated Supersymmetry Breaking, CERN TH/97–380 (hep–ph/9801271), to appear in Phys. Rep.; S. Ambrosanio, G.D. Kribs, S.P. Martin, Signals for gauge-mediated supersymmetry breaking models at the CERN LEP2 collider, Phys. Rev. D **56** (1997) 1761
2. ALEPH Collaboration, Searches for supersymmetry in the photon(s) plus missing energy channel at a centre-of-mass energy of 161 and 172 GeV, Phys. Lett. **B420** (1998) 127; ALEPH Collaboration, A study of single– and multi–photon production in e^+e^- collisions at a centre-of-mass energy of 183 GeV, Phys. Lett. **B427** (1998) 201
3. ALEPH Collaboration, Search for pair-production of long-lived heavy charged particles in e^+e^- annihilation, Phys. Lett. **B405** (1997) 379
4. ALEPH Collaboration, Search for sleptons in e^+e^- collisions at centre–of–mass energies up to 161 and 172 GeV, Phys. Lett. **B407** (1997) 377
5. ALEPH Collaboration, Search for sleptons in e^+e^- collisions at centre–of–mass energies up to 184 GeV, Phys. Lett. **B433** (1998) 176
6. ALEPH Collaboration, ALEPH: A detector for electron–positron annihilations at LEP, Nucl. Instrum. Methods A **294** (1990) 121
7. ALEPH Collaboration, Performance of the ALEPH detector at LEP, Nucl. Instrum. Methods A **360** (1995) 481
8. J.-F. Grivaz, F. Le Diberder, Complementary analyses and acceptance optimization in new particles searches, LAL preprint # 92–37 (1992); ALEPH Collaboration, Search for the standard model Higgs boson, Phys. Lett. B **313** (1993) 299
9. S. Dimopoulos, S. Thomas, J. D. Wells, Phys. Rev. **D54** (1996) 3283
10. R. D. Cousins, V. L. Highland, Nucl. Instrum. Methods **A320** (1992) 331

11. CDF Collaboration, Searches for New Physics in Diphoton Events in proton anti-proton collisions at sqrt(s)=1.8 TeV, Phys.Rev.Lett. **81** (1998) 1791-1796

12. ALEPH Collaboration, Searches for sleptons and quarks in e+e- collisions at 189 GeV, Phys. Lett. B **469** (1999) 303-314

13. ALEPH Collaboration, Searches for new particles in Z decays using the ALEPH detector, Phys. Rep. **216 (5-6)** (1992) 253; Search for the standard model Higgs boson, Phys. Lett. B **313** (1993) 299

14. LEP Collaborations, A combination of preliminary electroweak measurements and constraints on the Standard Model , CERN EP/99-015

15. ALEPH Collaboration, Search for Charginos and Neutralinos in e^+e^- collisions at $\sqrt{s}$=189 GeV and mass limit for the Lightest Neutralino, ALEPH99-011 CONF 99-006, paper in preparation

16. H. Baer, F. E. Paige, S. D. Protopopescu, X. Tata, ISAJET 7.40, a Monte Carlo Event Generator for pp, $p\bar{p}$ and e^+e^- Reactions, hep-ph/9810440

17. ALEPH Collaboration, Searches for the Neutral Higgs Bosons of the MSSM in e^+e^- collisions at centre-of-mass energies of 181-184 GeV, Phys. Lett. B **440** (1998) 419

18. J. Lopez, D. Nanopoulos, Phys. Rev. **D55** (1997) 4450